



Machinability improvement in Inconel-718 by enhanced tribological and thermal environment using textured tool

Chetan Darshan¹ · Sumit Jain² · Manu Dogra³ · Munish Kumar Gupta^{4,5} · Mozammel Mia⁶

Received: 23 September 2018 / Accepted: 15 February 2019 / Published online: 2 March 2019
© Akadémiai Kiadó, Budapest, Hungary 2019

Abstract

Machinability of Inconel-718 superalloy in conventional approach is poor—this fact necessitates advanced technological adoption such as improved surface topography over used cutting tool. Recently, the performance of textured tool has been investigated to explore its potential benefits in achieving favourability in machining of superalloy. In that context, the impact of tool texturing, cutting speed and machining time on some of the prominent machinability indices like cutting forces, tool wear, surface finish and chip morphology has been deliberately investigated. The performance comparison of non-textured and textured tool has been conducted at cutting speed of 80, 120 and 180 m min⁻¹ and at successive increment of machining times up to 10 min. Moreover, the scanning electron microscope analysis of worn tool edges was carried out to comprehend the wear mechanism. Furthermore, the thermal analysis was done for dedicated textured tooling condition. Results revealed that the textured tool performs better to ensure lower tool wear (V_B), reduced cutting forces (F_C), lower surface roughness (R_a) and acceptable form of chips. The spots of textured tool acted as fins to promote efficient heat transfer from cutting zone and reduced the effective chip–tool contact length to cause less friction.

Keywords Tribology · Inconel-718 alloy · Surface roughness · Textured tool · Tool wear

Introduction

Extensive utilization and demand of Inconel-718 superalloy in aviation, atomic reactor, chemical, food processing and marine industries are drawing much attention to the researchers, due to its unrivalled thermo-mechanical properties like high toughness, high tensile stress, rupture stress and resistance to degradation in corrosion and

oxidation [1, 2]. Since this alloy has significant industrial values in various applications, still the machining of Inconel-718 is considered to be very difficult [3]. Thick layer of adhesion and high thermal stress at the tool–workpiece interaction zone during cutting area result in poor thermal properties, propensity to severe work hardening and high tool–chip affinity, which represents several intrinsic characteristics [4]. For instance, tool becomes heated due to low thermal conductivity and heat flow towards it [5]. Moreover, the addition of Inconel-718 superalloy alloying elements into the tool diffuses the tool substrate and creates a thermal resistance and affects thermal conductivity; it further aggravates tool wear and these entire phenomenon forms a ‘vicious circle’ [6]. Recently, the cutting fluids and various tooling strategies have been generally used for enhancing the cutting tools performance during the machining of Inconel-718 and other superalloys. For instance, Sarikaya & Gullu, Sarikaya et al. and Yıldırım et al. implemented the minimum quantity cooling conditions for improving the machining performance of Waspaloy, Haynes 25, etc. [7–9]. The cutting fluids decreases the thermal wear on

✉ Chetan Darshan
chetandarshan@gmail.com

¹ IKGPTU, Jalandhar, Punjab, India

² MED, CTIEMT Shahpur, Jalandhar, Punjab, India

³ MED, SSG Regional Center, UIET Panjab University, Hoshiarpur, Punjab, India

⁴ University Center for Research and Development, Chandigarh University, Gharuan, Mohali, Punjab, India

⁵ Mechanical Engineering Department, National Institute of Technology, Hamirpur, India

⁶ Mechanical and Production Engineering, Ahsanullah University of Science and Technology, Dhaka, Bangladesh

geometric rake edge of the cutting insert and significantly improves the tool life [10–13]. But the cost of fluid supply system is high and conventional cutting fluids pose environmental and health risk for operators due to chemical disassociation of lubricant/coolant at high temperature, which motivates the researchers to find out the cheap and safe options for improving the machining performance of Inconel-718 alloy [14, 15].

Lately, the improvement in tool surface tribological characteristics by using micro-/nanoscale texturing has been widespread in machining of difficult-to-machine materials [16]. The texturing at tool rake surface acts as a micro-reservoir for lubrication and also provides a better machining characteristics in lieu of low cutting forces, good surface finish (R_a) and high tool life [17]. The generation of geometric patterns on the tool rake surface is done by adopting various methods, i.e. wire electrical discharge machining (WEDM), femtosecond laser, electrical discharge machining (EDM), micro-grinding, etc. [18]. Texture geometry such as parallel, perpendicular, cross-textured, elliptical and dimples, fabricated on tool rake face, also influences the tribological characteristics [19]. Elliptical and dimple-shaped textures enhanced tool performance by vast decrease in tool tip temperature, cutting forces and friction coefficient as compared to parallel and perpendicular textures [20]. Different researchers also proved that the type and shape of texturing significantly affect the machining performance [21–27]. In the first investigation, the execution of micro-scale pool lubricated cutting tool during machining mild steel is revealed by Lei et al. [21]. The texturing in the shape of micro-scale holes on rake surface of the tools was made by femtosecond laser. Similarly, Obikawa et al. [22] studied the impact of micro-scale textured (parallel and square dot type) tool while machining aluminium alloy A6061-T6 and found that micro-scale surfaces could develop the lubrication conditions adequately which cut down the cutting forces and energy intake. In similar work, Sugihara et al. [23] stated that adhesion at tool–chip while cutting the aluminium alloy (A5052) is overcome by generating micro-scale stripes on tool rake surface. Flood and dry environment are considered to test the performance of micro-scale stripe-textured cutting insert, which reveals improved cutting outcomes (e.g. anti-adhesive properties) of geometrically altered tool while machining aluminium alloy. Likewise, Xie et al. [24] utilized titanium alloy to compare the machining performance of textured and normal conventional tool under dry environment. They revealed that the cutting tool with texturing considerably reduces the cutting temperature up to 103 °C. In another work, Koshy and Tovey [25] used the isotropic textured tool (fabricated with the electrical discharge machining process) and revealed that micro-patterns on rake surface of tool

significantly reduce the feed and cutting forces. Ma et al. [26] explored the performance of micro-bump pattern on (WC/Co) uncoated cemented carbide insert in dry turning of mild steel (AISI 1045). The influence of texturing parameters, i.e. width, height and edge distance, was investigated concerning the cutting forces and tool–chip contact distance. In a similar context, Kim et al. [27] examined the impact of micro-pattern cubic boron nitride (CBN) inserts on the rake zone of tool via layer-by-layer EDM under various cutting conditions. They revealed that the micro-pattern inserts reduce the resulting force by 2.7 to 10.5% due to decrease in friction by 9.5 to 34.3% because they produce more shear and prevent abrasive wear as compared to non-pattern inserts by varying feed rate. Additionally, the wear on flank face was improved by 9.7 to 11.4% using micro-pattern inserts; however, the wear on crater zone contrasted little between the conventional and micro-patterned inserts. It was also clearly revealed that the contact area in machining zone decreases which dispenses the stress at the contact zone of tool–chip effectively, and therefore results in a less wear at the tool tip.

From the state-of-the-art review on current scientific works, it has been interestingly noticed that the texturing of tools is immensely being applied in machining of different materials like aluminium alloys, mild steels, etc. Besides, it has been observed from the literature that the texturing of tool at rake surface shows very promising outcomes as far as low cutting forces, good surface finish and high tool life. However, the holistic understandings of proper mechanisms of texturing tool during machining of Ni-based superalloys specifically Inconel-718 alloy are hardly discussed in the literature. Therefore, to fill this research gap, in the present work, the efforts are made on the texturing of uncoated carbide (WC/Co) tools and its applications in machining of Inconel-718 alloys at different process parameter conditions. For this purpose, the texturing of tool is done by laser micro-fabrication process, and initially, the influence of different cutting conditions, i.e. machining parameters and tooling strategies (textured and normal non-textured tool) on cutting forces, tool wear (crater and flank surface) and surface finish, has been experimentally investigated. Moreover, the scanning electron microscopy (SEM) is performed for in-depth analysis of tool wear pattern mechanisms during the machining of Ni-based superalloy (Inconel-718).

Materials and methods

Workpiece and cutting tool details

To perform the experiments, round bars of Inconel-718 (having axial length of 250 mm and diameter $\phi 26$ mm) are considered as subjected material. This superalloy is widely used in jet engine, gas turbine operations, nuclear reactors, etc. The workpiece round bar chemical composition is furnished in Table 1.

The uncoated carbide (WC/Co) tool, with ISO designation of TNMA 160408-THMF provided by Kennametal India Limited, was utilized for the machining tests. The tool was attached on a rigid tool holder with an ISO designation WTJNR1616H16, and it had 93° tool cutting edge angle.

Tooling strategies

Generally, the various methods of micro-fabrication are involved for material removal such as micro-grinding, micro-EDM, femtosecond laser and fibre laser, respectively. In this study, dimple-shaped texture having 50 μm diameter and 100 μm spacing is considered and is modelled with CAD software, as shown in Fig. 1a, b. The CAD model was then exported to suitable interface for fabricating texture on tool rake surface. Texture cluster on the tool rake surface of carbide insert was produced by a multi-diode pump fibre laser (LM-487-A-22-SD6-UX-M30-M) and the array of dimple texture is zigzag and the direction was parallel to cutting edge. The conventional insert with non-textured and dimple-textured pictures was measured by optical microscope and is displayed in Fig. 1a, b.

Machining tests

The dry machining tests on Inconel-718 were performed using conventional lathe (make: HMT, India, model: high-speed precision lathe NH 22 with specification: maximum power = 7.5 kW and maximum spindle speed = 2040 r.p.m). Initially, the peripheral layer ($\phi 26$ mm to $\phi 25$ mm) of subjected material is removed by uncoated carbide inserts to avoid machining of oxidized layer. Note that each

experimental test was conducted for time: 1–10 min progressively using a fresh cutting edge. The detailed cutting parameters adopted for machining tests are presented in Table 2. The cutting speed was varied at three levels, i.e. 80 m min^{-1} , 120 m min^{-1} and 180 m min^{-1} , and depth of cut and feed rate (f) are kept constant (i.e. 0.16 mm rev^{-1} and 0.5 mm , respectively). The experimental set-up is shown in Fig. 2.

Response measurements

In this work, the foremost machining outcomes such as arithmetic surface roughness (R_a), cutting forces, tool wear (V_b) and chip morphology were considered as per the ISO-9687 machining standard. For measurement of cutting forces, a three-component strain gauge-based dynamometer clamped under the tool rest (RMS controls) which was linked to a data acquisition and processing system has been used. Similarly, measurement of wear on flank surface of worn-out insert is done by Metzger, India, having magnification: $\times 30$ to $\times 150$ and $5\text{-}\mu\text{m}$ -resolution Toolmakers microscope. After executing the trials, the scanning electron microscope (SEM) has been used for cutting the tool edges. Then, the roughness profile of the machined specimens is assessed with a portable surface profile tester (Mitutoyo, SurfTest SJ-201, cut-off length = 0.8 mm). Lastly, the chips were visually inspected and analysed with respect to their shapes and size.

Mechanism of heat transfer in textured tools

In the machining of poor machinability materials, a thermal convection process is referred for transferring the heat from the cutting zone [19]. Generally, it is an energy transfer process that itself mixes the fluid medium, i.e. gases, liquids and powder. For textured tools, two types of heat exchange phenomenon take place: (1) transfer of fluid into empty space and (2) macro-form due to convection heat transfer. In natural or free convection, i.e. under dry conditions, buoyancy effects cause the circulation of heat because of density difference between hot and cold particles. As an example, consider that the heat is transferred

Table 1 Chemical composition of Inconel-718 alloy

Ni	Fe	Cr	Cu	Mo	Nb	C	Mn
50.00–55.00	Remainder	17.00–21.00	.30 max	2.80–3.30	4.75–5.50	.08 max	.35 max
P	S	Si	Ti	Al	Co	B	
.015 max	.015 max	.35 max	.65–1.15	.20–.80	1.00 max	.006 max	

Fig. 1 Optical microscope image at 50X. **a** Non-textured cutting tool with CAD model and **b** textured tool with CAD model

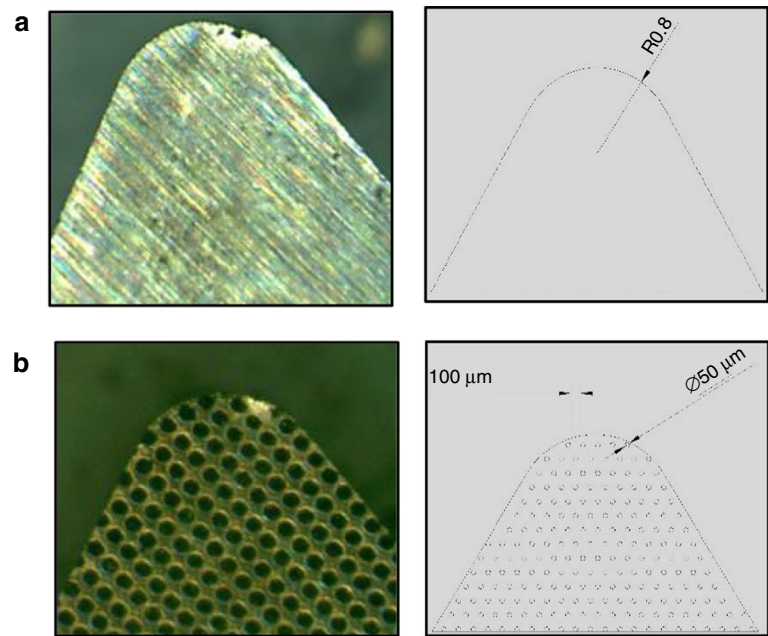


Table 2 Experimental conditions used in machining tests

Category	Specification
Workpiece material	Inconel-718 alloy
Work material size	Initial diameter = 26 mm Length = 250 mm
Cutting conditions	Cutting speed = 80, 120, 180 m min ⁻¹ Feed = 0.16 mm rev ⁻¹ Depth of cut = 0.5 mm Time = 1, 2, 4, 6, 8, 10 min
Cutting tool and tool geometry	TNMA 160408-THMF Rake angle (γ) = -6°, clearance angle (α) = 6°, nose radius = 0.8 mm
Machining environment	(i) Dry machining with uncoated carbide non-textured tool (NT) (ii) Dry machining with uncoated carbide textured tool (TT)

from the hot medium to environment with the mode of conduction. At the same time, the nearby stationary layer of air is heated by the conduction heat transfer. This exchanged energy is used to raise the temperature and boost up the internal energy. Consequently, the air becomes lighter with respect to the surrounding air. Expectedly the lighter air moves up forcing the heavier air to come down. In that interaction, the exchange of heat between cold and hot air takes place. This event is called convection, and mode of heat transfer is convection heat transfer, and its rate equation is shown in Eq. 1 (by Newton's law of cooling).

$$Q = hA(T_s - T_f) \quad (1)$$

where ' Q ' is the convection heat flow rate, ' h ' is the heat transfer coefficient, ' A ' is the active area for heat transfer, ' T_s ' is the surface temperature and ' T_f ' is the fluid temperature.

Let us consider the area of the surface of conventional tool as shown in Fig. 3a which behaves like a plate as $A_1 = 25$ sq. units. Then, the heat flow rate from the conventional tool is given by Eq. 2.

$$Q = hA_1(T_s - T_f) \quad (2)$$

Now, consider the surface area of the dimple-textured tool as shown in Fig. 3b. Removing the material from the plate surface with dimple texture reduces the area of the

Fig. 2 Experimental set-up with complete details

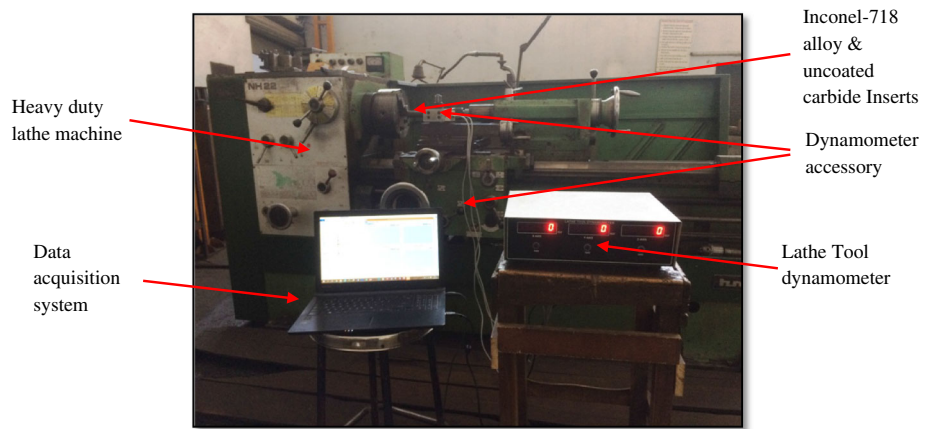


Fig. 3 Heat transfer concepts in textured tools

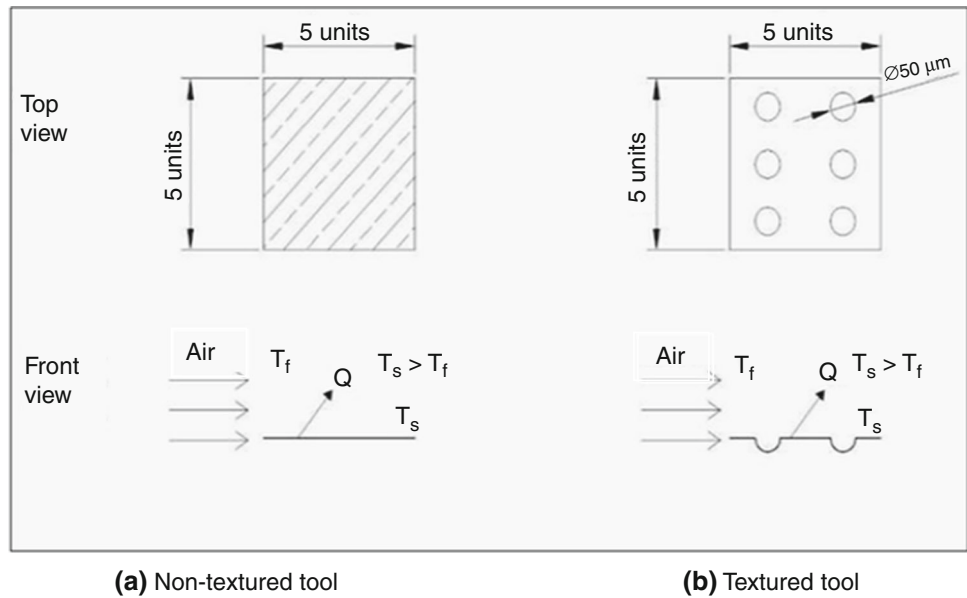


plate by A_2 , where A_2 is the area of circle on the surface of the plate shown in Eq. 3.

$$A_2 = n\pi r^2 \tag{3}$$

where r is the radius of the circle which is $25 \mu\text{m}$ and n is the number of circle. Therefore,

$$A_2 = 0.00785n \text{ sq. units}$$

The material is not removed from the plate surface to generate holes of radius r . Material is expelled to create the dimple texture on the surface and to expand the specific surface area of the plate which is in the shape of hemisphere. Therefore, the surface area of the hemisphere is given by A_3 ,

$$A_3 = 2n\pi r^2 \tag{4}$$

Considering the radius of the hemisphere as $25 \mu\text{m}$, then A_3 will be

$$A_3 = 0.0157n \text{ sq. units}$$

Hence, the heat flow equation of the cutting tool with dimple texture will be given by Eq. 5.

$$Q = h(A_1 - A_2 + A_3)(T_s - T_f) \tag{5}$$

After submitting the values of area A_1 , A_2 and A_3 , the equation is written as in Eq. 6.

$$Q = h(25 + 0.00785n)(T_s - T_f) \tag{6}$$

Equations (1) to (6) show that the surface area of the dimple-textured tool is higher as compared with conventional tools. Thus, the large amount of heat is flowed and transferred from the textured tools because heat flow rate is directly proportional to the specific surface area, i.e. the more the specific surface area, the more the heat carrying capacity of the cutting tool. Hence, the textured tools perform better as compared with the non-textured tool [19].

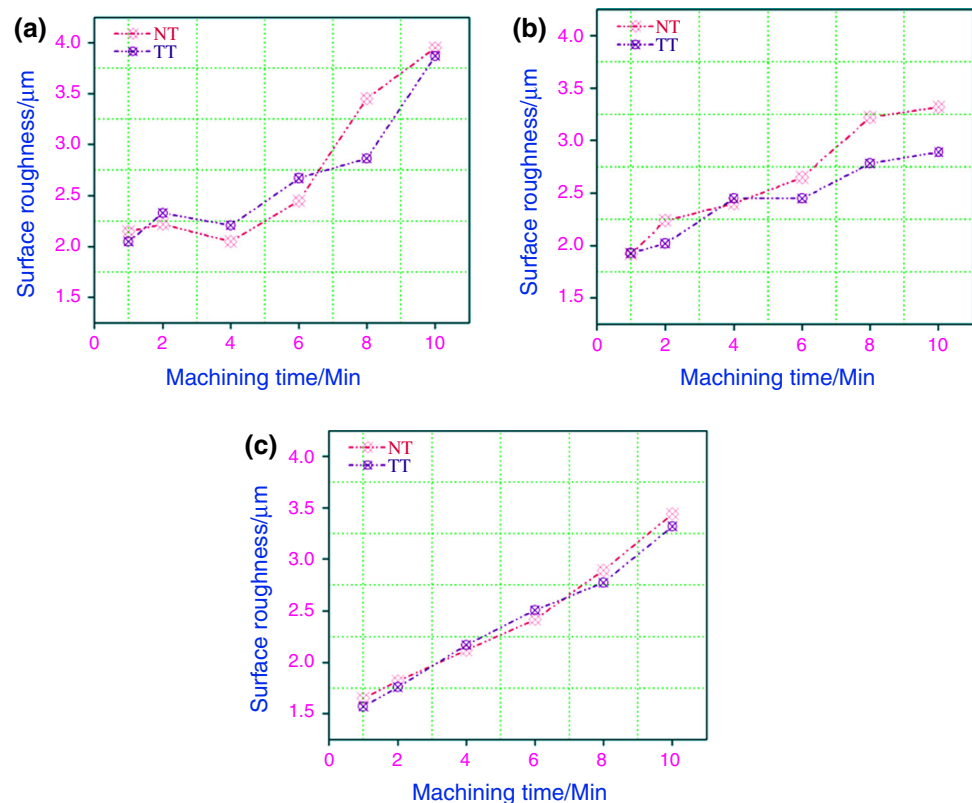
Results and discussion

Influence on surface roughness

Quality of the machined workpiece is assessed by its surface integrity characteristics. That said, the surface quality is determined largely by the cutting tool. The tribological performance at the tool–workpiece interface affects the service life and performance of cutting tool. The governing tribological phenomena are rubbing, friction, lubrication, stress, fatigue crack, etc. [25, 26]. Generally, the surface roughness is a quality evaluation criterion that refers to the high recurrence inconsistencies that are specifically related to the micro-structure, cutting actions and surface defects of materials [28–31]. The influence of textured tool (TT) and non-textured tools (NT) on surface roughness parameter (R_a) values w.r.t. cutting speed and machining time is presented in Fig. 4a–c. Figure 4 shows that the trend of surface roughness is increasing with the increase in machining time at all cutting speed values. The similar findings of surface roughness were stated by Gupta et al. [30] in turning of titanium alloy (grade 2) using MQL cooling strategy. This is due to the fact that during machining of hard-to-cut Ni-based superalloys, the high mechanical and thermal loading conditions cause some micro-structural and metallurgical alterations. Besides, the

poor thermal conductivity of aerospace materials such as Inconel-718 results in high-temperature handling zone, which influences tool wear and changes the cutting edge integrity; hence, the low surface finish was observed with the increase in machining time. The reason of this phenomenon is attributed to the three major factors that affect the surface roughness values: (1) built-up edge (BUE), (2) instigation of chip plastic side flow and (3) tool wear stability, respectively [32]. Moreover, it has been remarkably observed that the performance of conventional tool is better than the textured tool at starting interval of time, i.e. up to 6 min of machining time at 80 m min^{-1} (8.98% of improvement), 5 min at 120 m min^{-1} and 180 m min^{-1} . However, the performance of non-textured tool is deteriorating with the passage of time and the values of surface roughness are observed to be brought down on account of textured tools (by 17.10% of improvement). This may be associated with the basic concept of friction theories which stated that initially the friction coefficient is more in the case of textured tool (micro-scale texture was filled with wear debris), but as the time increases and up to a certain point the value of coefficient of friction starts decreasing because of the less chip–tool contact zone, and consequently, the value of surface roughness reduces after a certain point. Similarly, Sharma and Pandey [19] showed that the textured tool produces good surface finishing.

Fig. 4 Variation in surface roughness (in μm) at cutting speed of **a** 80, **b** 120, **c** 180 m min^{-1} w.r.t. machining time (min)



Besides, the friction generated at non-textured tool–chip interface plays the major role and has given the due consideration in increasing the surface roughness values at high cutting speed.

Influence on tool wear

With a specific end goal to comprehend the machining outcomes of any material, the tool wear rate must be evaluated. Surface quality, industrial cost and dimensional accuracy are influenced by tool wear. For processing difficult-to-machine aerospace components, cutting tool cost might be immaterial when contrasted with cost of work materials [33]. This section presents the in-depth analysis of tool wear pattern, i.e. flank wear in machining of Inconel-718 alloy with non-textured and textured tools. Generally, flank wear has been underscored more than crater wear for examining worn-out edge, because wear on flank surface and the resulting stagnation of the cutting edge have more direct impact on workpiece dimensions. The optical microscopic images at rake and flank surface of tools are displayed in Fig. 5. Similarly, the SEM analysis and tool wear patterns with respect to cutting speed and machining time are presented in Figs. 6–8.

Starting from the explanation of Fig. 5, it has been noticed that at cutting speed of 80 m min^{-1} the high work hardening tendency of Inconel-718 superalloy causes chipping and adhesion at outer edge of the cutting tool within short interval of time. The similar observations were reported by Sarikaya & Gullu, Sarikaya et al. and Yıldırım et al., in the machining performance of Waspaloy, Haynes 25 [7–9]. This is due to the basic phenomena that

the Inconel-718 is a hard but sticky material and high work hardening makes the machined surface of the Inconel-718 further hard, which results in an excessive stress on the outer edge of cutting edge causing chipping at the flank face within short time even when v_c is low, i.e. 80 m min^{-1} . Similarly, the mechanism of the tool wear at 120 and 180 m min^{-1} is subjected to the reason that the increase in cutting speed builds the specific cutting energy which is further converted into heat energy and causes material softening to be adhered as in the form of BUE. In fact, Mohanty et al. [34] observed the similar mechanisms during machining of aerospace material. However, Fig. 5 shows that machining with textured tool can attribute to the consolidated impact of speed and heat energy in the formation of abrasion and BUE. This is further stabilized and controlled by the high heat conduction rate due the micro-holes at the tool rake face. During machining with non-textured tool, big abrasion is visible ascribed to the dominant impact made by high cutting speed, as shown in Fig. 5.

After that, Figs. 6–8 clarify the trend of non-textured (NT) and textured (TT) tool on tool flank wear values at subjected conditions. It was clearly observed from the figures that the non-textured tool has more flank wear land width as compared with textured tools. Interestingly, this phenomenon is occurring at lower cutting speed as well as high cutting speed values while machining Inconel-718 alloy at different machining times. The justification of this mechanism is that at high cutting speed values the tool tip tends the chips to cover the rake face. However, the geometric alteration in terms of texturing on rake zone will act as micro-cutters, which reduce the tool–chip temperature

Fig. 5 Optical microscope images of worn faces of non-textured and textured tools at $\times 100$ magnification

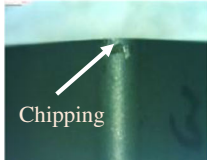
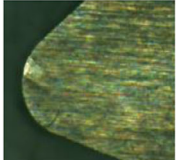
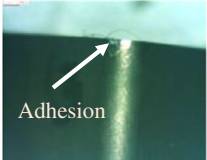
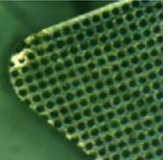
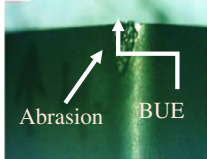


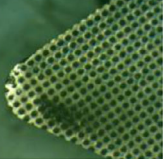
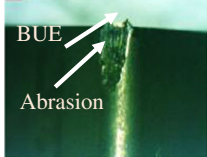
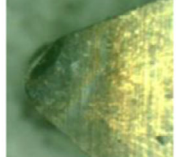

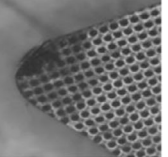
Cutting speed ↓	Machining conditions			
	Flank face of Non-textured tool (NT)	Rake face of Non-textured tool	Flank face of textured tool (TT)	Rake face of textured tool
80 m min^{-1}	 Chipping		 Adhesion	
120 m min^{-1}	 Abrasion BUE		 Abrasion	
180 m min^{-1}	 BUE Abrasion		 Abrasion	

Fig. 6 Variation in flank wear (in μm) at cutting speed of 80 m min^{-1} w.r.t. machining time (min)

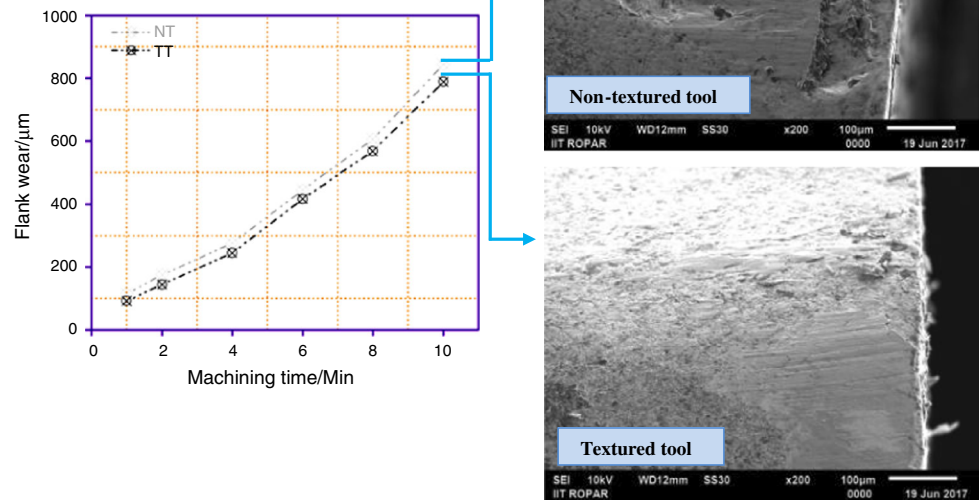
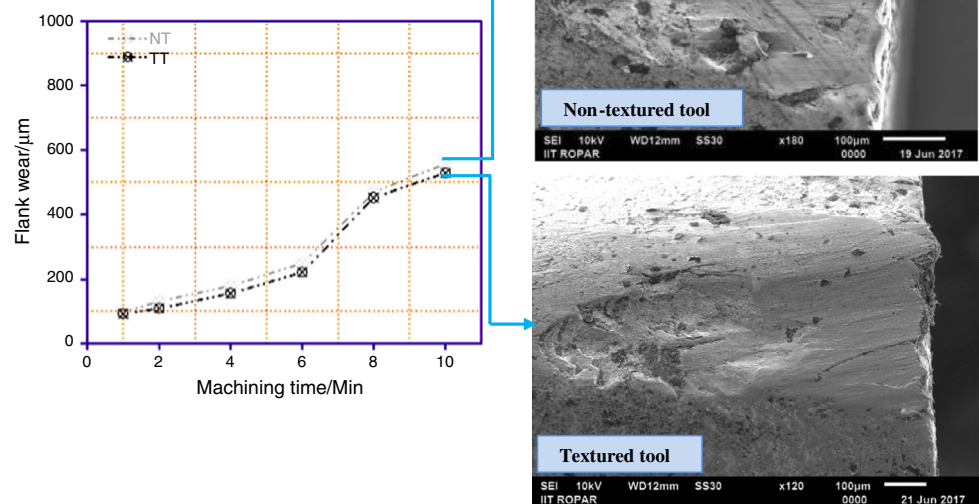


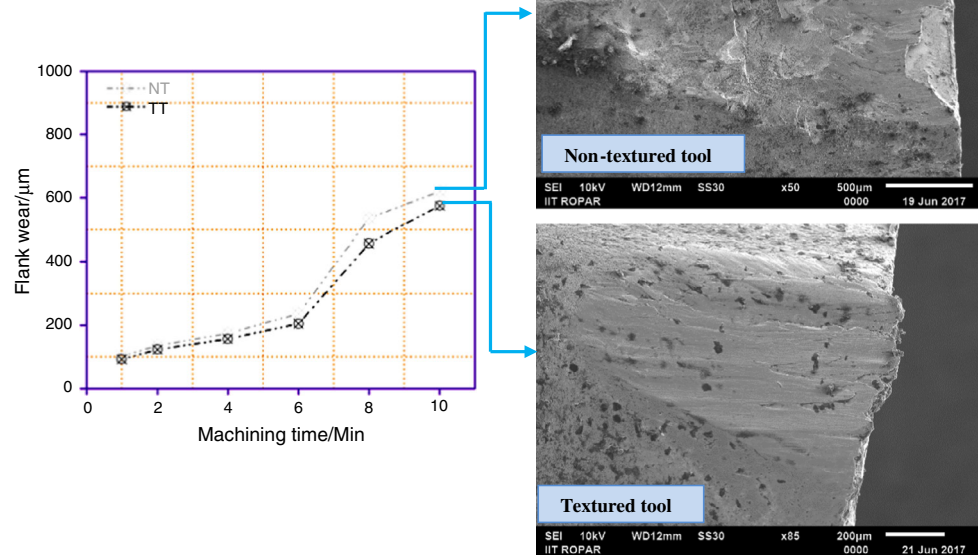
Fig. 7 Variation in flank wear (in μm) at cutting speed of 120 m min^{-1} w.r.t. machining time (min)



and lead to a shorter chip–tool contact distance resulting in a reduced tool wear. Besides, the BUE is stabilized in dimple-textured tool which resist the flank wear land width up to some extent, even at high cutting speed values. In addition, the geometric alteration in terms of texturing on rake zone improves the coefficient of friction by dropping adhesion and diffusion, and therefore reduces the forces

and temperature (discussed later). The similar facts were observed by Thomas and Kalaichelvan [16] in dry turning of high-speed steels. Furthermore, the texture on tool rake surface addresses the various issues and noticeably improves the tribological characteristics of cutting tool. The textured tool has empty zones under the surface that are loaded with air in dry cutting environment. These air

Fig. 8 Variation in flank wear (in μm) at cutting speed of 180 m min^{-1} w.r.t. machining time (min)



holes increase the shear deformation contrasted with a conventional (non-textured) tool, and the wear particles developed in tool–chip interface fall into the micro-scale cavity that helps to remove them from the contact zone. The micro-scale cavity at tool rake surface can prevent the abrasion wear.

Similarly, the justification of textured and non-textured tools in terms of SEM is presented here (i) Fig. 6, worn tools at 80 m min^{-1} , 5 (ii) Fig. 7, 120 m min^{-1} , 5 (iii) Fig. 8, 180 m min^{-1} . From this analysis, it has been observed that the dark-coloured spots are shown on the non-textured tools. These dark-coloured spots on the tool surface represent that the heat affected zone imprinted is by the thermal effect of friction at tool–chip interface. It was also observed that under dry condition flank wear rate increases rapidly by non-textured tools, whereas using textured tools the flank wear is reduced to 8.40%, 7.44% and 10.78% at 80 , 120 and 180 m min^{-1} , respectively. This reduction in tool flank wear is also attributed to the concept of heat transfer (natural convection), initially presented in the materials and methods section. Moreover, Figs. 6–8 show that the two main aspects, i.e. adhesion and chipping influences the tool flank wear land at lower cutting speed values of 80 m min^{-1} . With the increase in cutting speed, i.e. at 120 m min^{-1} , the flank land is worn out by dominating abrasion in non-textured tool and textured tool. However, at 180 m min^{-1} the tool face has been removed with abrasion and the inner core material of tool is revealed. In the end, it has been concluded that in all cutting conditions, the adhesion, abrasion, chipping and

BUE are found to be the governing wear patterns during turning of Inconel-718 alloy under dry conditions.

Influence on cutting forces

The discussion on cutting forces is of paramount importance since these factors directly affect the consumption of cutting power and machine tool structure [35]. Figure 9 illustrates the effect of textured and non-textured tools on axial thrust force F_x , radial thrust force F_y and main cutting force F_z as a function of cutting speed and machining time. Figure 9 shows that the textured tool under dry environment resulted in remarkable decrease in cutting forces as contrasted to the cutting forces produced in machining by non-textured tool. For instance, the axial thrust force (F_x) is decreased by 14.35%, 9.15% and 2.23% by using textured tool during machining at 80 , 120 and 180 m min^{-1} . Similarly, the radial thrust force (F_y) follows the same pattern and it decreased by 2.40%, 14.18% and 9.34%, respectively. In a similar context, the main cutting force (F_z) is decreased by 2.34%, 6.025% and 9.44% while machining with textured tool. Besides, the trend of the cutting forces is also well presented in Fig. 9. It clearly shows that the change in cutting speed at subjected conditions increases the cutting forces. The same trend of cutting forces was reported by Mehta et al. [36] during machining Inconel-718 alloy under sustainable environment. This is attributed to the basic phenomena that the high heat is generated with the implementation of non-textured tool and due to the poor thermal conductivity properties of Inconel-718 alloys

the heat is not transferred from the cutting zone. This generation of heat creates a thermal softening and higher stresses which further increases the friction and cutting forces. The concept of heat transfer is already explained, and the coefficient of friction is calculated with Eq. (7):

$$\mu = \tan(\beta) = \tan(\alpha + \arctan(F_y/F_z)) \quad (7)$$

where β represents the angle of friction, α is termed as rake angle, and F_y and F_z describes as radial thrust and main cutting force, respectively. Further, the contact area in tool–chip interfaces is less in the case of textured tools which therefore reduces the cutting forces as compared with the non-textured tool.

Influence on chip morphology

The whole machining dynamics is affected by the chip formation, and its analysis is very prominent for the evaluation of tool wear, cutting forces, roughness, etc. The entire knowledge regarding the various mechanisms, i.e. properties of material and distribution of stress during

deformation process, is available from the chip formation. The chip morphology is characterized with two aspects: (1) chip shape and (2) chip size, and these subjected characteristics are mostly affected by the friction between the tool–chip contact surfaces. For instance, the high friction at tool–chip interface formed large diameter curled chips and so on. Thence, in this work, the impact of cutting speed and machining time on chip morphology while machining Inconel-718 superalloy with non-textured and textured tool has been investigated. Figure 10 depicts the produced chips during machining Inconel-718 superalloy with non-textured and textured tool at given conditions. Interestingly, for non-textured tool the long serrated type chips are supposed to be generated owing to the unstable plastic deformation with adiabatic shear band (low thermal conductivity of Inconel-718). Conversely, the short spring types are produced while using textured tools. Initially, the large diameter curled and continuous kinds of chips were generated at low cutting speed of 80 m min^{-1} with non-textured tool. In case of textured tools, small segments of regular-size and spring-shaped chips are observed because

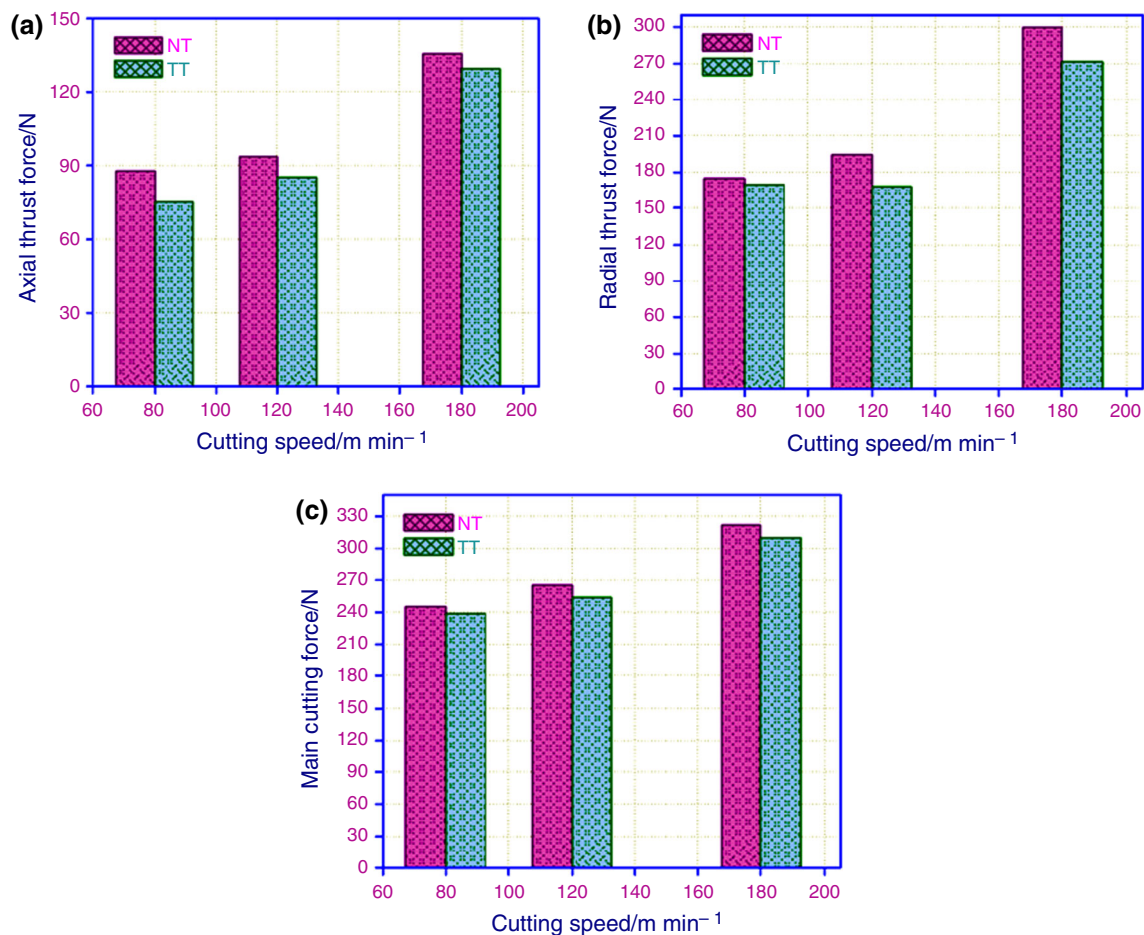
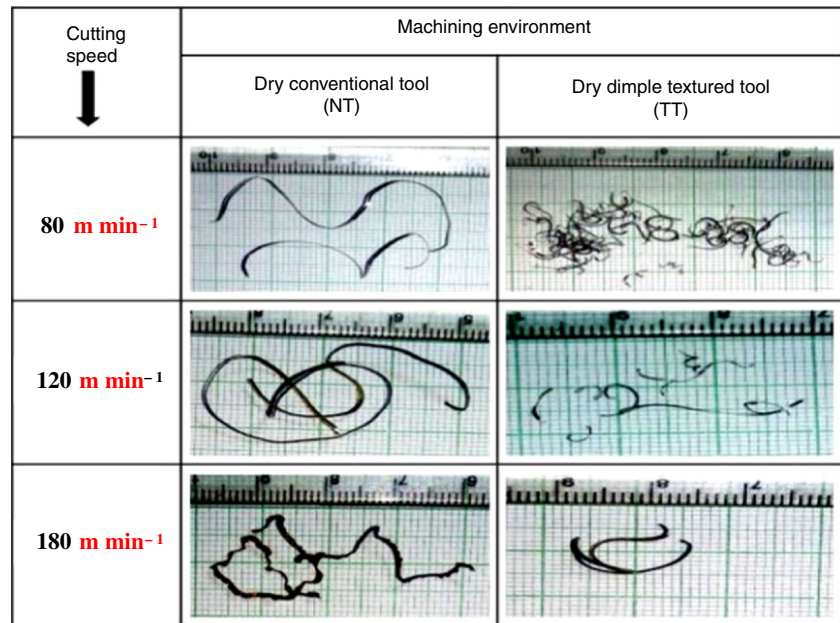


Fig. 9 Variation in cutting forces. **a** Axial thrust force F_x , **b** radial thrust force F_y , **c** main cutting force F_z

Fig. 10 Chips produced at cutting speed of 80, 120 and 180 m min⁻¹



grooves on the rake face act as a chip breaker which mainly reduced the tool–chip contact length; consequently, acceptable chips were produced. Further, the texturing on the rake face acts like chip breaker that reduced the curling diameter of the chips and deforms the chip plastically and breaks it down into the small segments. Up to cutting speed 120 m min⁻¹, continuous straight chips with serrated edges and small sawtooth were formed in case of non-textured tool, which are not broken timely and it may have adverse impact on surface finish and rise in temperature in cutting zone. Sharma and Pandey [19] also observed the similar findings with non-textured tools. Moreover, an increase in cutting speed produces the intense shear band on a recently formed chip surface which ends up with less chip width as compared to chip that were produced at 80 m min⁻¹. However, in case of textured tool, smooth segments of chips are formed because textured tool act as chip breaker, but the segments of chip are somewhat larger as compared to non-textured tool at 80 m min⁻¹. At higher speed of 180 m min⁻¹, due to high temperature in shear zone and cutting zone, the golden colour continuous chips with large sawtooth are produced during machining with non-textured tool. The use of textured tool reduces the contact surface and as a result continuous coiled segmented chips with large chip thickness have been produced.

Conclusions

In this work, the turning tests on Inconel-718 superalloy have been performed with non-textured and textured tools. The fibre laser method has been used for generating dimple

texture on rake surface of tool. In parallel, the influence of machining conditions and different tools has been investigated on prominent machining indices. Based upon these experimental findings, the following conclusions were summarized:

1. For surface roughness measurements: Surface quality in terms of roughness is lower as cutting speed and time increase. This is generalized concept that the Inconel-718 alloy is a low thermal conductivity material that results in generation of excessive temperature at cutting zone. This high temperature highly affects the tool wear and edge integrity, thereby resulting in low values R_a with increase in machining time and cutting speed.
2. For tool wear: The increase in cutting speed and machining time demonstrated the larger values of tool flank wear. Also, the texturing on cutting tool provides the good lubricating action at tool–chip interface and hence reduces the tool flank wear values as compared with non-textured tools.
3. From SEM: The adhesion, abrasion, chipping and BUE are found to be the most dominating wear mechanisms during machining of Inconel-718 alloy under dry conditions.
4. For cutting force estimation: The three components of cutting forces are increased with the change in cutting speed from 80 to 180 m min⁻¹. Moreover, it has been noted that the cutting forces produced with the textured tools are much lesser than the non-textured tools. Actually, the surface area of textured tool is higher than the non-textured tool, and as a result, more heat is

flowed over the rake face of cutting tool. Hence, the less friction is generated, and therefore, less cutting forces are produced with textured tools.

5. Chip morphology: During the machining of Inconel-718 alloy, two types of chips, i.e. serrated type long and spring type short chips have been produced with normal and textured tools.
6. Lastly, it has been concluded that use of dimple-textured tool during machining of Inconel-718 alloys shows very positive results. This is valid as the textured tools significantly improve the machining performance of Inconel-718 alloy by reducing cutting forces, tool wear and surface roughness.

Future work

The implementations of environmental cooling strategies such as minimum quantity lubrication conditions, cryogenic cooling, high-pressure cooling and nano-fluids conditions with the application of textured tools are some future outlooks of research.

Compliance with ethical standards

Conflict of interest The authors declare that they have no conflict of interest.

References

1. Bansal A, Sharma AK, Das S, Kumar P. On microstructure and strength properties of microwave welded Inconel 718/stainless steel (SS-316L). *Proc Inst Mech Eng Part L J Mater Des Appl.* 2015;230:939–48. <https://doi.org/10.1177/1464420715589206>.
2. Bhopale NN, Pawade RS, Joshi SS. Surface quality analysis in ball end milling of Inconel 718 cantilevers by response surface methodology. *Proc Inst Mech Eng Part B J Eng Manuf.* 2015;231:628–40. <https://doi.org/10.1177/0954405415600140>.
3. Unune DR, Mali HS. Experimental investigation on low-frequency vibration-assisted μ -ED milling of Inconel 718. *Mater Manuf Process.* 2018;33:964–76. <https://doi.org/10.1080/10426914.2017.1388516>.
4. Singh G, Gupta MK, Mia M, Sharma VS. Modeling and optimization of tool wear in MQL-assisted milling of Inconel 718 superalloy using evolutionary techniques. *Int J Adv Manuf Technol.* 2018;97:481–94. <https://doi.org/10.1007/s00170-018-1911-3>.
5. Moon S-H, Lee C-M. A study on the machining characteristics using plasma assisted machining of AISI 1045 steel and Inconel 718. *Int J Mech Sci.* 2018;142–143:595–602.
6. Antonialli AÍS, Magri A, Diniz AE. Tool life and tool wear in taper turning of a nickel-based superalloy. *Int J Adv Manuf Technol.* 2016;87:2023–32. <https://doi.org/10.1007/s00170-016-8568-6>.
7. Sarıkaya M, Güllü A. Multi-response optimization of minimum quantity lubrication parameters using Taguchi-based grey relational analysis in turning of difficult-to-cut alloy Haynes 25. *J Clean Prod.* 2015;91:347–57.
8. Yıldırım ÇV, Kıvak T, Sarıkaya M, Erzincanlı F. Determination of MQL parameters contributing to sustainable machining in the milling of nickel-base superalloy waspaloy. *Arab J Sci Eng.* 2017;42:4667–81. <https://doi.org/10.1007/s13369-017-2594-z>.
9. Sarıkaya M, Yılmaz V, Güllü A. Analysis of cutting parameters and cooling/lubrication methods for sustainable machining in turning of Haynes 25 superalloy. *J Clean Prod.* 2016;133:172–81.
10. Anamalai K, Samyalingam L, Kadirgama K, Samykano M, Najafi G, Ramasamy D, et al. Multi-objective optimization of the machining parameters for bio-inspired nanocoalant. *J Therm Anal Calorim.* 2018. <https://doi.org/10.1007/s10973-018-7693-x>.
11. Mia M. Multi-response optimization of end milling parameters under through-tool cryogenic cooling condition. *Measurement.* 2017;111:134–45.
12. Gupta M, Pruncu C, Mia M, Singh G, Singh S, Prakash C, et al. Machinability investigations of Inconel-800 super alloy under sustainable cooling conditions. *Materials (Basel).* 2018;11:2088.
13. Mia M, Singh G, Gupta MK, Sharma VS. Influence of Ranque-Hilsch vortex tube and nitrogen gas assisted MQL in precision turning of Al 6061-T6. *Precis Eng.* 2018;53:289–99.
14. Mia M, Gupta MK, Singh G, Królczyk G, Pimenov DY. An approach to cleaner production for machining hardened steel using different cooling-lubrication conditions. *J Clean Prod.* 2018;187:1069–81.
15. Mia M, Morshed MS, Kharshiduzzaman M, Razi MH, Mostafa MR, Rahman SMS, et al. Prediction and optimization of surface roughness in minimum quantity coolant lubrication applied turning of high hardness steel. *Measurement.* 2018;118:43–51.
16. Jesudass Thomas S, Kalaichelvan K. Comparative study of the effect of surface texturing on cutting tool in dry cutting. *Mater Manuf Process.* 2018;33:683–94. <https://doi.org/10.1080/10426914.2017.1376070>.
17. Dinesh S, Senthilkumar V, Asokan P. Experimental studies on the cryogenic machining of biodegradable ZK60 Mg alloy using micro-textured tools. *Mater Manuf Process.* 2017;32:979–87. <https://doi.org/10.1080/10426914.2016.1221096>.
18. Thiyagu M, Karunamoorthy L, Arun Kumar N. Magnetorheological fluid-based nanotexturing of tool inserts for turning of duplex stainless steel. *Mater Manuf Process.* 2017;32:1019–25. <https://doi.org/10.1080/10426914.2016.1257136>.
19. Sharma V, Pandey PM. Comparative study of turning of 4340 hardened steel with hybrid textured self-lubricating cutting inserts. *Mater Manuf Process.* 2016;31:1904–16. <https://doi.org/10.1080/10426914.2015.1127951>.
20. Arulkirubakaran D, Senthilkumar V, Kumawat V. Effect of micro-textured tools on machining of Ti–6Al–4V alloy: an experimental and numerical approach. *Int J Refract Met Hard Mater.* 2016;54:165–77.
21. Lei S, Devarajan S, Chang Z. A study of micropool lubricated cutting tool in machining of mild steel. *J Mater Process Technol.* 2009;209:1612–20.
22. Obikawa T, Kamio A, Takaoka H, Osada A. Micro-texture at the coated tool face for high performance cutting. *Int J Mach Tools Manuf.* 2011;51:966–72.
23. Sugihara T, Enomoto T, Yukinaga S. Improving tool wear resistance in steel cutting by textured surface and its mechanism. *Adv Mater Res.* 2012;565:424–9.
24. Xie J, Luo MJ, Wu KK, Yang LF, Li DH. Experimental study on cutting temperature and cutting force in dry turning of titanium alloy using a non-coated micro-grooved tool. *Int J Mach Tools Manuf.* 2013;73:25–36.

25. Koshy P, Tovey J. Performance of electrical discharge textured cutting tools. *CIRP Ann.* 2011;60:153–6.
26. Ma J, Duong NH, Lei S. Numerical investigation of the performance of microbump textured cutting tool in dry machining of AISI 1045 steel. *J Manuf Process.* 2015;19:194–204.
27. Kim DM, Lee I, Kim SK, Kim BH, Park HW. Influence of a micropatterned insert on characteristics of the tool–workpiece interface in a hard turning process. *J Mater Process Technol.* 2016;229:160–71.
28. Gupta MK, Sood PK, Sharma VS. Investigations on surface roughness measurement in minimum quantity lubrication turning of titanium alloys using response surface methodology and Box-Cox transformation. *J Manuf Sci Prod.* 2016;16:75–88.
29. Mia M, Dhar NR. Influence of single and dual cryogenic jets on machinability characteristics in turning of Ti–6Al–4V. *Proc Inst Mech Eng Part B J Eng Manuf.* 2017;233:711–26. <https://doi.org/10.1177/0954405417737581>.
30. Gupta MK, Sood PK, Sharma VS. Machining parameters optimization of titanium alloy using response surface methodology and particle swarm optimization under minimum-quantity lubrication environment. *Mater Manuf Process.* 2016;31:1671–82. <https://doi.org/10.1080/10426914.2015.1117632>.
31. Gupta MK, Sood PK. Surface roughness measurements in NFMQL assisted turning of titanium alloys: an optimization approach. *Friction.* 2017;5:155–70.
32. Ferreira R, Carou D, Lauro CH, Davim JP. Surface roughness investigation in the hard turning of steel using ceramic tools. *Mater Manuf Process.* 2016;31:648–52. <https://doi.org/10.1080/10426914.2014.995051>.
33. Delahaigue J, Chatelain J-F, Lebrun G. Machining analysis of unidirectional and bi-directional flax-epoxy composite laminates. *Proc Inst Mech Eng Part L J Mater Des Appl.* 2017;231:196–209. <https://doi.org/10.1177/1464420716671970>.
34. Mohanty A, Gangopadhyay S, Thakur A. On applicability of multilayer coated tool in dry machining of aerospace grade stainless steel. *Mater Manuf Process.* 2016;31:869–79. <https://doi.org/10.1080/10426914.2015.1070413>.
35. Madyira DM, Laubscher RF, van Rensburg NJ, Henning PFJ. High speed machining induced residual stresses in Grade 5 titanium alloy. *Proc Inst Mech Eng Part L J Mater Des Appl.* 2012;227:208–15. <https://doi.org/10.1177/1464420712462319>.
36. Mehta A, Hemakumar S, Patil A, Khandke SP, Kuppan P, Oyyaravelu R, et al. Influence of sustainable cutting environments on cutting forces, surface roughness and tool wear in turning of Inconel 718. *Mater Today Proc.* 2018;5:6746–54.

Publisher's Note Springer Nature remains neutral with regard to jurisdictional claims in published maps and institutional affiliations.